

field, Mass. 01535.

<sup>17</sup>J. DeKlerk, in *Physical Acoustics*, edited by W. P. Mason (Academic, New York, 1966), Vol. 4A, p. 195.

<sup>18</sup>M. Pomerantz, *Phys. Rev.* **139**, A501 (1965).

<sup>19</sup>M. Pomerantz, *Proc. IEEE* **53**, 1438 (1965).

<sup>20</sup>P. C. Kwok, *Phys. Rev.* **149**, 666 (1966).

<sup>21</sup>M. Pomerantz, *Phys. Rev. B* **1**, 4029 (1970).

<sup>22</sup>M. Dutoit, thesis, Washington University, 1970

(unpublished).

<sup>23</sup>W. P. Mason, in *Physical Acoustics*, edited by W. P. Mason (Academic, New York, 1966), Vol. 4A, p. 299.

<sup>24</sup>M. Pollak and T. H. Geballe, *Phys. Rev.* **122**, 1742 (1961).

<sup>25</sup>S. Tanaka and H. Y. Fan, *Phys. Rev.* **132**, 1516 (1963).

PHYSICAL REVIEW B

VOLUME 3, NUMBER 2

15 JANUARY 1971

## Application of the Method of Tight Binding to the Calculation of the Energy Band Structures of Diamond, Silicon, and Sodium Crystals\*

Roy C. Chaney† and Chun C. Lin

*Department of Physics, University of Wisconsin, Madison, Wisconsin 53706*  
and

Earl E. Lafon

*Department of Physics, Oklahoma State University, Stillwater, Oklahoma 74074*  
(Received 29 July 1970)

The method of tight binding is used to calculate the energy band structure of the diamond, silicon, and sodium crystals. The wave functions of the valence and conduction bands of diamond are expanded in terms of Bloch sums constructed from the 1s, 2s, and 2p Hartree-Fock atomic orbitals, and two different crystal potentials [the muffin-tin and the overlapping atomic potential (OAP)] were used. With the muffin-tin potential, the tight-binding and the augmented-plane-wave (APW) method yield nearly identical valence band structure, and their conduction bands show only minor differences. When the OAP is used, the results of the tight-binding scheme differ appreciably from those of Bassani and Yoshimine by the method of orthogonalized plane waves (OPW), the discrepancy being attributed to incomplete convergence of the latter calculations. The tight-binding structures of the valence band derived from the two different potentials agree quite well with each other, but considerable deviations are found in the conduction band. The x-ray form factors calculated by means of the tight-binding wave functions are in good agreement with experiment and represent a considerable improvement over a simple superposition of atomic charges. The convergence of the tight-binding method with respect to the higher atomic orbitals has been examined. It is found that addition of 3s, 3p, and 3d Bloch sums to the wave functions of diamond has only small effects on the energy of the valence and conduction bands. A similar tight-binding calculation has been performed for the band structure of silicon using OAP, and the results are in good agreement with those of a modified scheme of the method of OPW using as basis functions 609 OPW's as well as the Bloch sums of the core states. For the case of sodium, the method of tight binding gives conduction-band energies in good agreement with the APW-type calculations of Schlosser and Marcus. Generalization of the method of tight binding by using single-Gaussian Bloch sums is discussed, and the use of this scheme leads to substantial improvements for the case of diamond.

### I. INTRODUCTION

A few years ago it was shown that the method of tight binding for calculating electronic energy band structure of crystals, which, hitherto, was used largely for qualitative purposes, is capable of giving energies in very good agreement with those obtained by methods based on modified plane-wave-type expansion.<sup>1</sup> The difficulty of evaluating the multicenter integrals, which had been the bottleneck of any quantitative application of the method of tight binding, was circumvented by the use of the Gaussian transformation. In a more

recent paper,<sup>2</sup> it was pointed out that if the atomic wave functions were expressed in terms of the Gaussian-type orbitals (instead of the Slater-type orbitals), all the multicenter integrals occurring in the band-structure calculations can be reduced to analytic forms, and the computational procedure is greatly simplified.

In both Refs. 1 and 2, we have seen that when the overlap between atomic wave functions at all sites are properly taken into consideration and the summation over the crystal sites in the computation of matrix elements is carried out to convergence, the method of tight binding is even applicable

to the case of lithium crystals where the valence electrons behave more like free particles than ones specifically attached to an individual atom. The success of the tight-binding method for even the case of loosely bound electrons suggests that it should certainly be applicable to the insulator-type crystals. In order to test the applicability of this method to wider classes of crystals and to extend the calculations to crystals of the second-row elements, we have used the tight-binding method to calculate the energy band structures of diamond, silicon, and sodium. Since the major interest is to study the method of tight binding as a means of accurate calculations of the energies of a one-electron Hamiltonian with a given periodic potential, comparison of our result is made mainly with the results computed by other methods using the same potential. For a critical comparison of the theoretical band structure with experiment, it is more appropriate to use the self-consistent-field-type (SCF) calculations; indeed, comparisons of this kind have been made for diamond and silicon.<sup>3-6</sup> Since our calculations are not of the SCF type and the crystal potentials used here are based on the overlapping-atomic-potential (OAP) model or the muffin-tin type, no attempt is made to conduct a systematic comparison of our calculated band structure with experiments. In this paper we confine ourselves to discussions of the general utility of the tight-binding method for solving one-electron periodic-potential problems. A logical extension is to incorporate the SCF scheme into the tight-binding method.

At this point it may be advisable to say a few words about the terminology used in this paper, since some confusions appear to exist as to the precise meaning of the term *tight binding*. The *method of tight binding* as used in this work, as well as in Refs. 1 and 2, refers to the scheme of calculating electronic energy bands of crystals by the use of Bloch sums, e.g., those given in Eq. (4) of Ref. 1, as basis functions. The results of Refs. 1 and 2, however, have demonstrated that the method of tight binding is applicable even to *loosely bound* electrons. Thus the name of the tight-binding method may be somewhat misleading, and the method of linear combination of atomic orbitals (LCAO) may be a more appropriate designation. Nevertheless we continue to use the term "method of tight binding" interchangeably with the term "method of LCAO" (the latter being more preferable when one wishes to emphasize the special feature of expressing the wave functions of electrons in crystals in terms of the electron wave functions of the constituent atoms). The so-called "tight-binding approximation" sometimes is taken to mean the approximation of neglecting all the multicenter integrals except those involving

atomic orbitals situated at two nearest-neighbor sites in calculations using the method of tight binding. This "tight-binding approximation" was never used here or in our earlier works, and, in fact, it would have led to unsatisfactory results for lithium as we have demonstrated in Refs. 1 and 2.

For tight-binding calculations one can use atomic wave functions expressed in terms of either the Slater-type orbitals (STO) or the Gaussian-type orbitals (GTO). The latter, however, offers a very substantial reduction of the computational procedure especially when the number of basis functions becomes larger. All the calculations reported in this paper, with the exception of those described in Secs. II E and V, were performed using the STO. Development of special techniques to achieve higher accuracy of the energy calculations for the Gaussian-basis scheme is under way, and a detailed report will be published elsewhere.

## II. DIAMOND

### A. Crystal Potential

The diamond lattice can be thought of as being constructed from two interpenetrating sublattices of face-centered cubic (fcc) structure which we will designate here as sublattices 1 and 2. Each lattice site of the second sublattice is separated from the corresponding member of the first by the nonprimitive translation  $\vec{T}$  directed, along the body diagonal of the face-centered cube of the first sublattice and of magnitude  $\frac{1}{4}\sqrt{3}a_0$  where  $a_0$  is the lattice constant of the sublattice. We will place the origin of our coordinate system at a point midway between these sublattices and with axes parallel to the edges of the face-centered cubes. The Wigner-Seitz cell situated about the origin has a volume  $\Omega = \frac{1}{4}a_0^3$  and contains two atoms at locations given by

$$\vec{t}_1 = -\frac{1}{2}\vec{T} = -\frac{1}{8}a_0(1, 1, 1) = -\vec{t}_2 \quad (1)$$

for sublattices 1 and 2, respectively. The atoms in adjacent cells are given by  $\vec{R}_\nu \pm \frac{1}{2}\vec{T}$ , where  $\vec{R}_\nu$  is the set of symmetry translations for the fcc lattice. The corresponding reciprocal lattice is generated by  $\vec{K}_\nu$  and is seen to be body-centered cubic. The crystal potential of diamond is invariant under inversion about the above origin and can thus be represented by the Fourier series

$$V_{\text{cry}}(\vec{r}) = \sum_\nu V_{\text{cry}}(\vec{K}_\nu) \cos \vec{K}_\nu \cdot \vec{r} \quad (2)$$

Alternatively, the crystal potential can be expressed mathematically as a superposition of functions  $v(\vec{r})$  centered about the atomic sites of the crystals, i.e.,

$$V_{\text{cry}}(\vec{r}) = \sum_\nu \{v[\vec{r} - (\vec{R}_\nu + \vec{t}_1)] + v[-\vec{r} + (\vec{R}_\nu + \vec{t}_2)]\} \quad (3)$$

Taking the  $\psi(\vec{r})$  as spherically symmetrical, the Fourier coefficients of the potential are given by

$$V_{\text{cryst}}(\vec{K}_\nu) = (N\Omega)^{-1} \int V_{\text{cryst}}(\vec{r}) \cos \vec{K}_\nu \cdot \vec{r} d\tau \\ = 2\Omega^{-1} \cos \vec{K}_\nu \cdot \vec{t}_1 \int \psi(r) \cos \vec{K}_\nu \cdot \vec{r} d\tau, \quad (4)$$

where  $N$  represents symbolically the number of unit cells of the crystal. We have calculated the band structure of diamond with two choices of potential, each of which will be described briefly.

The first choice is that of a muffin-tin potential as reported for diamond by Keown.<sup>7</sup> In this particular muffin version developed by Mattheiss,<sup>8</sup> the crystal is divided into regions by spheres of radius  $R_{IS} = |\vec{t}_1|$  centered about each of the carbon atoms. Within each sphere, an atomlike potential  $V'(r)$  is constructed by approximating the crystal charge density with a spherically averaged sum of overlapping free-atom charge distributions and by applying the Slater approximation for exchange.<sup>9</sup> In the region between the spheres, the potential is treated as a constant  $\bar{V}$  whose value is either determined by an averaging process or is treated as a disposable parameter.<sup>10</sup> In the potential of Keown,  $\bar{V}$  was treated as a parameter and set equal to  $-1.3928$  Ry. For such a potential,  $\psi(r)$  can be expressed mathematically as the sum of two contributions

$$\psi(r) = \psi^{(1)}(r) + \psi^{(2)}(r), \quad (5)$$

where

$$\psi^{(1)}(r) = V'(r) - \bar{V} \quad \text{for } r \leq R_{IS} \\ = 0 \quad \text{for } r > R_{IS}, \quad (6) \\ \psi^{(2)}(r) = \frac{1}{2} \bar{V} / N.$$

The value of  $a_0$  used in connection with this potential is 6.7406 a.u.

The second choice of potential, sometimes called the overlapping-atomic-potential (OAP) model,<sup>11,12</sup> approximates the crystal potential by a sum of free-atom potentials using the Slater approximation for exchange on each atomic charge distribution separately. It is convenient to introduce the free-atom charge density  $\rho(r)$  which is obtained from the Hartree-Fock SCF solution of Jucys<sup>13</sup> for the  $(1s)^2(2s)^2(2p)^2$  ground state<sup>14</sup> of carbon by the relation

$$4\pi\rho(r) = 2[R_{1s}(r)]^2 + 2[R_{2s}(r)]^2 + 2[R_{2p}(r)]^2. \quad (7)$$

We can decompose  $\psi(r)$  into the part due to the Coulomb interaction of the nucleus and the electrons plus the exchange contribution which is approximated by  $-\frac{3}{2}[3\rho(r)/\pi]^{1/3}$  in Hartree atomic units. The Fourier coefficients then become

$$V_{\text{cryst}}(\vec{K}_\nu) = -8\pi K_\nu^{-2} \Omega^{-1} \cos(\vec{K}_\nu \cdot \vec{t}_1) \\ \times \left[ Z - K_\nu^{-1} \int_0^\infty 4\pi r \rho(r) \sin(K_\nu r) dr \right. \\ \left. + K_\nu \int_0^\infty \frac{3}{2} r \left( \frac{3\rho(r)}{\pi} \right)^{1/3} \sin(K_\nu r) dr \right], \quad (8)$$

where  $Z$  is the atomic number. To carry out the above integration, we curve fit  $r\rho(r)$  and  $r[\rho(r)]^{1/3}$  to a three-term and a five-term linear combination of the type  $r^a e^{-br}$ , respectively, by a nonlinear least-squares process. The value of  $a_0$  for this potential was chosen to be 6.728 a.u. to facilitate comparison with the calculation of Bassani and Yoshimine<sup>15</sup> by the method of orthogonalized plane waves (OPW).

One may, of course, question the validity of using a muffin-tin potential for covalent crystals. This point has been discussed by Keown and Wood.<sup>16</sup> Nevertheless, both types of potential have been investigated here by tight binding in order to perform a comprehensive comparison between the band structures calculated by different methods, e.g., the method of augmented plane waves (APW) with the muffin-tin potential<sup>7</sup> and OPW with the OAP model.<sup>15</sup>

#### B. Tight-Binding Calculations

The Hartree-Fock SCF atomic wave functions of the 1s, 2s, and 2p states of carbon are obtained by fitting the tabulated functions of Jucys<sup>17</sup> for the  $^5S$  state of the  $(1s)^2(2s)(2p)^3$  configuration as

$$\phi_{1s} = 1.79382 e^{-8.33500r} + 6.00411 e^{-5.28343r}, \\ \phi_{2s} = 1.71115 e^{-5.11268r} - 1.28779r e^{-1.70623r}, \quad (9) \\ \phi_{2px} = x(1.69606 e^{-2.64212r} + 0.840266 e^{-1.28884r}),$$

etc.

The five Bloch sums corresponding to 1s, 2s, 2px, 2py, 2pz can then be constructed for each of the two sublattices making a total of ten basis functions in all. However, rather than employing these Bloch sums directly, we find it convenient to form linear combinations analogous to "bonding" and "antibonding" at the  $\Gamma$  point, i.e.,

$$b_\alpha^*(\vec{k} \cdot \vec{r}) = I^*(\alpha) N^{-1/2} \sum_\nu e^{i\vec{k} \cdot \vec{R}_\nu} [\phi_\alpha(\vec{r} - \vec{R}_\nu - \vec{t}_1) \\ \pm \phi_\alpha(\vec{r} - \vec{R}_\nu - \vec{t}_2)], \quad (10)$$

where

$$\alpha = 1s, 2s, 2px, 2py, 2pz,$$

and

$$I^*(\alpha) = -i\Gamma(\alpha) = 1, \quad \alpha = ns \\ = i, \quad \alpha = np_x, np_y, np_z. \quad (11)$$

This step is not essential but does serve to simplify the calculation of the energy at the  $\Gamma$  point and to make the matrix elements of the secular equation formed from these ten Bloch sums real.

For a general point in the Brillouin zone, the ten basis functions in Eq. (10) lead to the usual  $10 \times 10$  secular equation. Analogous to Ref. 1, the elements of the secular determinant  $|H - ES|$  consist of the overlap, kinetic-energy, and potential-energy integrals which can be decomposed into a number of multicenter integrals and evaluated in a manner similar to that described for the case of lithium.<sup>1</sup> The only significant exception is that the point  $C$  in Ref. 1, which represents the origin of the Fourier expansion of potential, no longer coincides with an atomic position but specifies a point midway between two carbon atoms. The resultant Fourier frequency integrals which must be evaluated are

$$\langle \psi^s(A) | \cos \vec{K}_v \cdot \vec{r}_C | \phi^s(B) \rangle$$

with  $\psi^s(A)$  and  $\phi^s(B)$  being *unnormalized* STO situated at points  $A$  and  $B$ , respectively, whereas the corresponding integrals in Ref. 1 are of the form

$$\langle \psi^s(A) | \cos \vec{K}_v \cdot \vec{r}_A | \phi^s(B) \rangle.$$

Following the procedure described in Ref. 1, we obtain

$$\begin{aligned} \langle \psi^s(A) | \cos \vec{K}_v \cdot \vec{r}_C | \phi^s(B) \rangle &= 2\pi \sum_i \beta_i \int_0^1 \gamma_i(u) \\ &\times \left( \sum_{n=0}^7 \mu_{i,n} (fg)^{-(9-n)/2} \right) \end{aligned}$$

$$\begin{aligned} &\times e^{-(fg)^{1/2}} \{ \xi_{i,1} \cos[\vec{K}_v \cdot (\vec{r}_{CB} - u\vec{r}_{AB})] \\ &+ \xi_{i,2} \sin[\vec{K}_v \cdot (\vec{r}_{CB} - u\vec{r}_{AB})] \} du, \end{aligned} \quad (12)$$

where

$$\begin{aligned} f &= u(1-u)r_{AB}^2, \\ g &= K_v^2 + \alpha_2^2/(1-u) + \alpha_1^2/u, \end{aligned} \quad (13)$$

and the coefficients  $\beta_i$ ,  $\gamma_i(u)$ ,  $\mu_{i,n}$ , and  $\xi_{i,j}$  are given in Table I of Ref. 1. The overlap and kinetic-energy integrals can be obtained directly from Eqs. (19) and (20) of Ref. 1.

With these methods of decomposition into multicenter integrals, the secular equation for a given  $\vec{k}$  can be constructed and solved. The two lowest roots correspond to "core" states, the remaining eight roots are separated equally into valence and conduction states. Some of the band energies obtained in this manner are presented in Table I for both the muffin-tin potential and OAP. The atomic multicenter integrals mentioned above need be evaluated only once for each crystal problem as they are independent of the choice of  $\vec{k}$ . Thus, once these integrals have been determined, the energies associated with any given point in the Brillouin zone are easily obtained.

As would be expected from the relatively open nature of the diamond lattice, the convergence of the energy matrix elements for diamond, with respect to the inclusion of more and more sets of nearest neighbors, was a great deal more rapid than was the case for lithium. Indeed, all ten eigenvalues of the secular equation were found to stabilize after all sets of neighbor atoms were

TABLE I. Comparison of band structure of diamond calculated by different methods with different potentials (in a.u.).<sup>a</sup>

	TB OAP <sup>b</sup>		OPW SCF-PERT	OPW OAP	APW Muffin-tin	TB Muffin-tin <sup>b</sup>	
	10 × 10	20 × 20				10 × 10	20 × 20
$\Gamma_1$	-0.740	-0.743	-0.772	-0.845	-0.720	-0.709	-0.704
$\Gamma'_{25}$	0.0	0.0	0.0	0.0	0.0	0.0	0.0
$\Gamma'_{15}$	0.230	0.229	0.254	0.203	0.215	0.198	0.212
$\Gamma'_2$	0.494	0.491	0.518	0.496	0.392	0.389	0.406
$X_1$	-0.435	-0.446	-0.460	-0.515	-0.422	-0.409	-0.418
$X_4$	-0.204	-0.217	-0.206	-0.255	-0.191	-0.178	-0.199
$X_1$	0.311	0.296	0.221	0.146	0.219	0.253	0.259
$X_3$	0.595	0.597	0.768		0.524	0.507	0.520
$L'_2$	-0.549	-0.553	-0.562	-0.637	-0.528	-0.518	-0.519
$L_1$	-0.424	-0.452	-0.456	-0.530	-0.426	-0.401	-0.429
$L_4$	-0.095	-0.100	-0.074	-0.197	-0.087	-0.082	-0.091
$L_1$	0.371	0.368	0.357	0.296	0.291	0.301	0.311
$L_3$	0.371	0.368	0.390	0.173	0.316	0.318	0.332
$L'_2$	0.658	0.653	0.684	0.296	0.525	0.558	0.563

<sup>a</sup>In this table the energy of  $\Gamma'_{25}$  is set to zero. The energy values of  $\Gamma'_{25}$  calculated by the tight-binding method are -0.503 (10 × 10) and -0.505 (20 × 20) using the OAP model, and are -0.417 (10 × 10) and -0.431 (20 × 20) with the muffin-tin potential.

<sup>b</sup>TB refers to tight binding.

included which lay within a sphere of radius  $2.5a_0$  about the origin. The corresponding number for lithium is  $6a_0$ .

In Eq. (9) we express each atomic SCF wave function as a linear combination of two STO. The relative weighting coefficients were determined by solving the atomic SCF problem. In a crystal, these weighting coefficients are expected to change; hence we may treat them as unknown coefficients to be fixed by the variational principle and thereby improve the accuracy of the energy values. The band structures resulting from this extension are plotted in Figs. 1 and 2 for the muffin-tin potential and OAP, respectively, and numerical values of the energy for selected points in the Brillouin zone are included in Table I. The crystal energies derived from this  $20 \times 20$  secular equation are all slightly lower than those from the original  $10 \times 10$ . This procedure of extending the basis functions does not require any new integrals, and in fact, the computational scheme is no more complicated than the case of fixed weighting coefficients except for an increase in size of the energy matrix.

With the OAP model, the resultant indirect band gap is calculated to be of magnitude 5.3 eV in good agreement with the experimental value<sup>18</sup> of 5.47 eV, while the associated minimum of the conduction band is calculated to lie at  $k = (2\pi/a_0)(0.58, 0, 0)$  compared with an experimental value of  $(2\pi/a_0)(0.75, 0, 0)$ .<sup>19</sup> As can be seen in Fig. 2, the minimum of the conduction band is a very shallow one and thus very accurate calculations are needed to locate it.

### C. Comparison of Different Calculations

In order to compare the accuracy of the various methods for solving the problem of periodic potential, it is important that the same crystal potential be used in all cases. In comparing the accuracy, one may keep in mind that since our tight-binding calculation is based on the linear

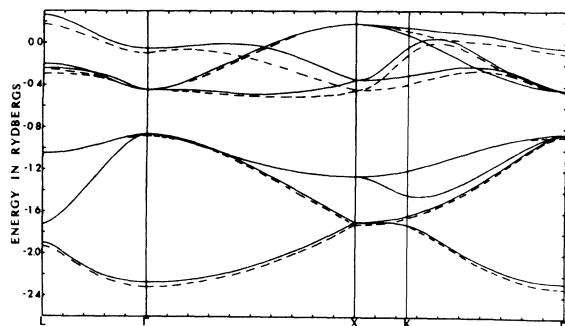


FIG. 1. Energy band structure of diamond with muffin-tin potential. Solid curves were calculated by the tight-binding method and the dashed curves by APW.

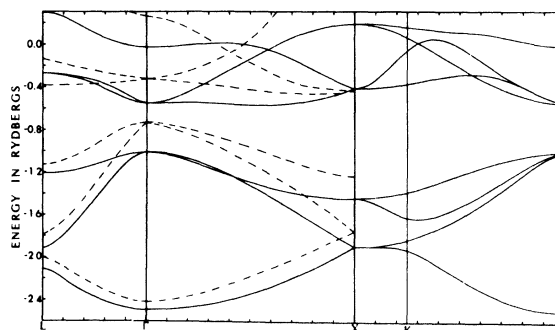


FIG. 2. Energy band structure of diamond with the OAP. Solid curves were calculated by the tight-binding method and the dashed curves by OPW.

variation method, the calculated energies constitute the upper limit of the corresponding true eigenvalues for the given periodic-potential problem. Figure 1 shows a comparison between the APW and the tight-binding calculation ( $20 \times 20$  secular equation) using the same muffin-tin potential. The two sets of results agree well in the valence band, but a somewhat larger discrepancy is seen in the conduction band. In view of the high precision of the APW calculation, this discrepancy can be taken as a measure of the accuracy of our tight-binding energies. In Sec. V we will show how to improve tight-binding results and indeed reduce the disagreement with the APW work.

In Fig. 2 we include both the tight-binding and OPW energies<sup>15</sup> which result from the OAP model. At almost every point in the Brillouin zone the tight-binding energies are substantially below the OPW results, indicating the higher accuracy of the former. The major discrepancy between the two sets of energies is most probably due to incomplete convergence of the OPW expansion.

Table I lists the energies of diamond at a number of high-symmetry points in the Brillouin zone as calculated by several different methods with different crystal potentials ( $\Gamma_{25}$  being set equal to zero). Because of the iterative nature of the SCF calculations, the crystal potential which was used to obtain Herman's results of the "perturbed SCF" calculation<sup>3,4</sup> is somewhat different from the OAP model. The empirical adjustment of the SCF energies to fit experimental data, as made by Herman, further changes the energy values, typically by an amount of 1 eV. While the close agreement between the OAP tight-binding calculation with Herman's work is not to be taken as a test of the accuracy of the tight-binding method *per se*, the similarity of the two sets of band structure obtained by two different schemes of computation does add some measures of the reliability of the calculated band structures. In addition to the *ab initio* calcu-

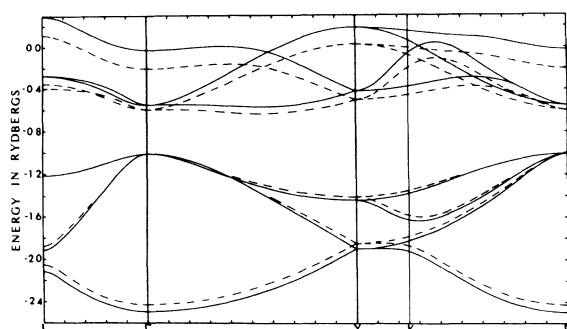


FIG. 3. Energy band structure of diamond calculated by the tight-binding method. The solid curves were obtained by using the OAP model and the dashed curves by the muffin-tin potential. The energies computed from the muffin-tin potential were shifted by a constant amount in order to bring the two sets of curves to coincidence at the top of the valence band.

lations cited above, studies of the band structure of diamond by empirical schemes have been made.<sup>20</sup> In view of the vast basic differences of motivation and procedure between the first-principle and the empirical schemes, detailed comparison of their results will not be made here.

At this point it is instructive to compare the tight-binding band structures calculated by the two different potentials, i.e., muffin-tin potential and OAP. This is illustrated in Fig. 3. The two sets of curves agree very well in the valence band. In the conduction band, however, one notices a much more pronounced difference in the band shape of the two cases as well as an over-all shift of energy

of about 0.7 eV. It has been pointed out that the direct band gap ( $\Gamma_{15} - \Gamma'_{25}$ ) varies considerably with the magnitude of the parameter  $\bar{V}$ ,<sup>16</sup> thus the shift of the conduction-band curves may be ascribed to the particular value of  $\bar{V}$  chosen by Keown in constructing his muffin-tin potential.

To compare the Fourier coefficients of the OAP and muffin-tin potential, we show in Fig. 4 the variations of  $-(K_v^2 \cos \vec{K}_v \cdot \vec{t}) V_{\text{cry}}(\vec{K}_v)$  versus  $K_v^2$  for these two potentials. Included in this graph are also the Fourier amplitudes of another muffin-tin potential in which the value of  $\bar{V}$  is chosen so as to make  $V_{\text{cry}}(r)$  continuous at the boundaries of the inscribed sphere. This continuous muffin-tin potential differs from the OAP only in the low-frequency components and converges to OAP in the high-frequency region which governs the atomic-like potential of the core. The muffin-tin potential of Keown, on the other hand, exhibits considerable oscillation at high frequencies which may be ascribed to the discontinuity at the surface of the inscribed sphere. This oscillation has much faster damping than what appears in Fig. 4 since the ordinate is proportional to  $K_v^2 V_{\text{cry}}(\vec{K}_v)$  rather than  $V_{\text{cry}}(\vec{K}_v)$  itself.

#### D. Calculation of X-Ray Form Factors

In addition to the question of the accuracy of the energy band structure produced by tight binding, it is also desirable to obtain some indication as to the nature of the wave functions associated with various eigenvalues in the Brillouin zone. For diamond we have attempted to evaluate the overall accuracy of the wave functions by obtaining from them the band-structure charge density which

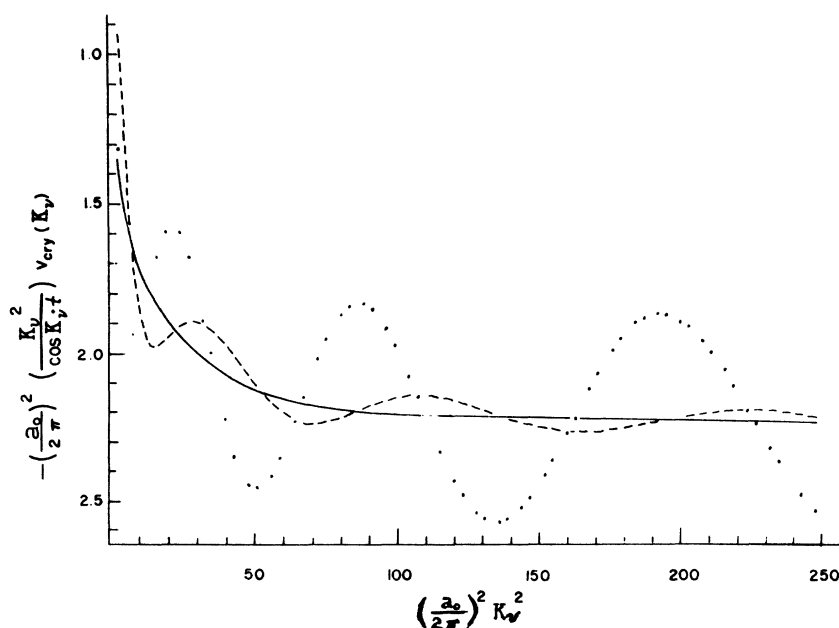


FIG. 4. Fourier coefficients of the crystal potentials; dotted curve for Keown's muffin-tin potential, solid curve for OAP. The dashed curve corresponds to the muffin-tin potential which is continuous at the boundaries of the inscribed sphere.

can be compared directly with other calculations and with experiment. In our investigation of the charge density of diamond, a three-point quadrature of the occupied states of the Brillouin zone was performed using the points  $\Gamma$ ,  $X$ , and  $L$  with a relative weighting of 1:3:4, respectively. The details of the calculation are presented elsewhere<sup>21</sup> and will not be repeated here. A graph of the total electronic charge density along the  $[111]$  direction is shown in Fig. 5 (solid line). For comparison, the charge density which would result from simply superposing spherical free-atom charge distributions centered about the various lattice sites in the crystal is also presented in Fig. 5 (dashed line). The most obvious feature of this graph is the shift of charge into the region of the covalent bond. The Fourier components of the contribution of the valence electrons to the electronic charge density is presented in units of electrons/atom in Table II. Two other calculations<sup>22,23</sup> as well as the experimental results of Göttlicher and Wölfel<sup>24</sup> are also presented for comparison. As can be seen, the LCAO results are in quite good agreement with experiment and represent a considerable improvement over a naive superposition of atomic charges. Even without using SCF wave functions, over one-half of the forbidden reflection is accounted for, and it is hoped this agreement can be further improved by carrying out the solutions of the one-electron wave functions to self-consistency.

#### E. Inclusion of Higher Atomic Orbitals

To carry the method of tight binding further, one

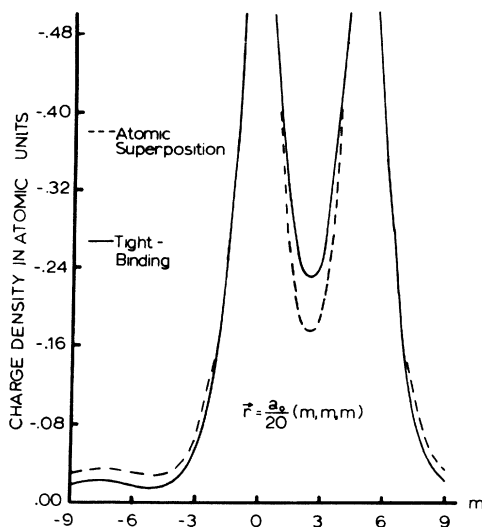


FIG. 5. Electronic charge density along the  $[111]$  direction of the crystal. The solid curve was obtained from the tight-binding functions and the dashed curve by superposition of spherical free-atom charge distribution.

TABLE II. Comparison of various calculations of Fourier components of valence charge density in diamond (units of electrons/atom).

$(2\pi/a_0)$ $(l_x, l_y, l_z)$	$sp^3$ super- position	Tight binding	GK <sup>a</sup>	RESC <sup>b</sup>	Expt <sup>c</sup>
111	0.814	0.93	1.011	0.976	0.99
220	0.203	0.16	0.221	0.15	0.18
311	0.045	-0.02	-0.037	-0.05	-0.04
222	0.0	-0.08	-0.105	-0.12	$\pm 0.15$
400	-0.013	-0.06	-0.105	-0.10	-0.14
331	0.018	0.01	0.029	0.02	0.02
442	0.028	0.03	0.084	0.06	0.02
333	0.018	0.02	0.085	0.06	0.00
511	0.018	0.02	0.054	0.04	0.00

<sup>a</sup>Reference 22.

<sup>b</sup>Reference 23. The Fourier coefficients listed here differ from those given in Ref. 23 in that the expansion is performed about the inversion center midway between the two atoms rather than about an atomic site.

<sup>c</sup>Reference 24.

can construct the Bloch sums corresponding to the higher orbitals such as  $3s$ ,  $3p$ ,  $3d$ , and expand the crystal wave functions by all these Bloch sums,

$$\psi(\vec{k}, \vec{r}) = \sum_{nlm} [a_{nlm}^*(\vec{k}) b_{nlm}^*(\vec{k}, \vec{r}) + a_{nlm}(\vec{k}) b_{nlm}(\vec{k}, \vec{r})]. \quad (14)$$

Although no rigorous test has been performed, the convergence of the above expansion was generally assumed when one includes only the Bloch sums of the atomic orbitals corresponding to the occupied shells of the free atoms. This convergence is borne out by the good agreement of the results of both diamond reported here and lithium in our previous work (in which only  $1s$ ,  $2s$ , and  $2p$  orbitals were used) with energy bands calculated by other methods. It has been suggested by Parmenter<sup>25</sup> that because of the long range of the higher atomic orbitals, the Bloch sums formed by them are approximately identical except for a multiplicative constant. To examine the convergence behaviors more quantitatively, we have included the Bloch sums of the  $3s$ ,  $3p$ , and  $3d$  orbitals in the expansion of Eq. (14). The wave functions of the  $3s$ ,  $3p$ , and  $3d$  states of the free carbon atoms were obtained by the Hartree-Fock-Slater SCF procedure.<sup>26</sup> With the increased number of basis functions, in order to simplify the computational procedures, the atomic wave functions are now expressed as linear combinations of GTO in this calculation. The  $1s$  and  $2s$  functions were taken from the nine-term and the  $2p$  from the five-term expansions of Huzinaga's work.<sup>27</sup> The  $3s$ ,  $3p$ , and  $3d$  Hartree-Fock-Slater functions were curve fitted to

$$\phi_{3s} = \sum_j \beta_{s,j} e^{-\alpha_j r^2},$$

$$\begin{aligned}\phi_{3px} &= x \sum_j \beta_{p,j} e^{-\alpha_j r^2}, \quad \text{etc.}, \\ \phi_{3dxy} &= xy \sum_j \beta_{d,j} e^{-\alpha_j r^2}, \quad \text{etc.},\end{aligned}\quad (15)$$

where  $\alpha_j$  are 146.097, 42.4974, 14.1892, 5.14773, 1.96655, 1.14293, 0.359450, 0.153310, 0.114600, 0.0214306, 0.0199309, 0.0194012; the associated  $\beta_{s,j}$  are 0.127873, 0.0919759, 0.180825, 0.0699163, 0.128500, -0.136868, -0.0493034, -0.115833, 0.0745720, 0.0404171, 0, 0; the associated  $\beta_{p,j}$  are -0.0991902, 0.296303, 0.00252251, 0.319199, -0.0563510, 0.227016,

0.00725878, 0.0718979, -0.0588483, 0, -0.00947948, 0; and the associated  $\beta_{d,j}$  are 0.00401002, 0.0143208, 0.00947481, 0.0176495, 0.00854137, 0.0135360, 0.0174888, -0.00726030, 0.0116090, 0, 0, -0.00254764. The use of GTO for tight-binding calculations has been discussed.<sup>2</sup> The kinetic-energy, potential-energy, and overlap matrix elements between *s* and *p* orbitals can be found in Ref. 2, and those involving the *d*-type orbitals can be obtained by the usual differentiation technique. For example, following the notation of Ref. 2, we have

$$\begin{aligned}&\langle G^{d(3x^2-r^2)}(\alpha_1, \vec{r}-\vec{A}) | \cos \vec{K}_v \cdot \vec{r}_c | G^s(\alpha_2, \vec{r}-\vec{B}) \rangle \\ &= \frac{1.5}{\alpha_1} \frac{\partial}{\partial \alpha_1} \langle G^{ps}(\alpha_1, \vec{r}-\vec{A}) | \cos \vec{K}_v \cdot \vec{r}_c | G^s(\alpha_2, \vec{r}-\vec{B}) \rangle \left( \frac{1.5}{\alpha_1} + \frac{\partial}{\partial \alpha_1} \right) \langle G^s(\alpha_1, \vec{r}-\vec{A}) | \cos \vec{K}_v \cdot \vec{r}_c | G^s(\alpha_2, \vec{r}-\vec{B}) \rangle, \quad \text{etc.}\end{aligned}\quad (16)$$

With only the Bloch sums constructed from the Huzinaga 1s, 2s, and 2p Gaussian-type atomic orbitals, we obtain the same band structure as those resulting from the use of the Slater-type wave functions. When the basis set is extended to include the 3s, 3p, and 3d Bloch sums, the band energy is suppressed slightly from the values derived from the 1s-2s-2p set. For  $k=0$ , the energies (with OAP model) of  $\Gamma_1$ ,  $\Gamma'_{25}$ ,  $\Gamma_{15}$ , and  $\Gamma'_2$  are -1.266, -0.512, -0.280, and -0.022 a.u., respectively, for the former case, and are -1.243, -0.503, -0.273, and -0.009 a.u., respectively, for the latter. Thus the higher orbitals, indeed, are of very minor importance for the energies of the valence and conduction bands. As one proceeds in the expansion of Eq. (14) to orbitals of higher  $n$ , the Bloch sums become nearly identical to each other and, hence, entirely ineffective for improving the crystal wave functions. In Sec. V we shall discuss a different scheme for augmenting the basis set.

### III. SILICON

#### A. Tight-Binding Calculations

Because of the similarity in the crystal structure, the procedure for band-structure calculations of silicon follows closely to that of diamond. For the crystal potential we use only the OAP model calculated from the SCF atomic wave function of the  $(1s)^2(2s)^2(2p)^6(3s)^2(3p)^2$  configuration given by Clementi<sup>26</sup> with a lattice constant  $a_0 = 10.26$  a.u. The Fourier coefficients of this potential agree well with the corresponding ones given by Bassani and Yoshimine.<sup>15</sup> The selection of the basis set here is not as clear cut as in the case of the first-

row element crystals. It is obvious that one must include the Bloch sums of the atomic states up to 3s and 3p. In fact, they constitute the minimal basis set in that we can construct from them basis functions of all symmetry species of the valence band. On the other hand, it may be desirable to use all the atomic orbitals in the occupied valence shell which include 3d in addition to 3s and 3p. To investigate this point we have calculated the band structure using the minimal set as well as the one which includes 3d. The SCF wave functions of the 1s, 2s, 2p, 3s, and 3p states of silicon have been given in terms of the STO.<sup>28</sup> We calculated the 3d function by the Hartree-Fock-Slater scheme and curve fit the radial part to the form

$$\begin{aligned}R_{3d}(\text{Si}) &= 0.818899 e^{-4.08524r} + 0.374280 e^{-7.81297r} \\ &+ 0.208879 e^{-1.09340r} + 0.197731 e^{-1.86255r}.\end{aligned}$$

Expressions for integrals involving the 3s, 3p, and 3d STO can be deduced again by the standard differentiation technique which will not be presented here. Comparisons of the energies at several high-symmetry points of the Brillouin zone computed by the two different basis sets may be found in Table III. One may notice rather substantial differences at the  $X_1$ ,  $L_3$ , and  $L'_2$  points. The band structure resulting from the 1s-to-3d basis set is illustrated in Fig. 6. We obtain the indirect band gap of 1.8 eV in reasonable agreement with the experimental value<sup>29</sup> of 1.13 eV. The calculated minimum of the conduction band lies at  $(2\pi/a_0)(0.8, 0, 0)$  as compared to  $(2\pi/a_0)(0.85, 0, 0)$  from experiment.<sup>30</sup>



TABLE III. Comparison of the energies (in a.u.) of silicon calculated by the  $1s-2s-2p-3s-3p$  and by the  $1s-2s-2p-3s-3p-3d$  basis set under the tight-binding scheme.

	Energies			Energies	
	$1s3p$	$1s3d$		$1s3p$	$1s3d$
$\Gamma_1$	-0.829	-0.829	$X_3$	-0.030	-0.048
$\Gamma'_{25}$	-0.400	-0.414	$L'_2$	-0.757	-0.757
$\Gamma'_2$	-0.325	-0.325	$L_1$	-0.636	-0.643
$\Gamma_{15}$	-0.281	-0.294	$L_4$	-0.445	-0.453
$X_1$	-0.689	-0.692	$L_1$	-0.330	-0.346
$X_4$	-0.495	-0.501	$L_3$	-0.203	-0.257
$X_1$	-0.294	-0.342	$L'_2$	0.002	-0.040

#### B. Comparison with OPW Method

Although there have been many calculations of band structure of Si, most of the first-principle results are by the OPW method. Thus a detailed comparison of the tight-binding and the OPW band structure is made here. The potential used in the tight-binding calculations of silicon was constructed to be identical to that used by Bassani and Yoshimine in their OPW work.<sup>15</sup> Comparison between these two calculations is shown in Fig. 6. As can be seen, the tight-binding results lie considerably below those of OPW, thus we judge the tight-binding calculations to be considerably more accurate than the OPW calculations of Bassani and Yoshimine using some 90 OPW's.

In order to obtain a more realistic estimate of the accuracy of the tight-binding method, we have performed a slightly modified OPW calculation using some 609 plane waves. In the usual OPW formalism, the core states which are obtained by solving the atomiclike problem in the crystal or by the use of "core shifts," are assumed to be eigenstates of the Hamiltonian. If the core functions used in forming the OPW do not accurately represent the true core eigenstates, the OPW solutions do not converge to the exact eigenvalues of the

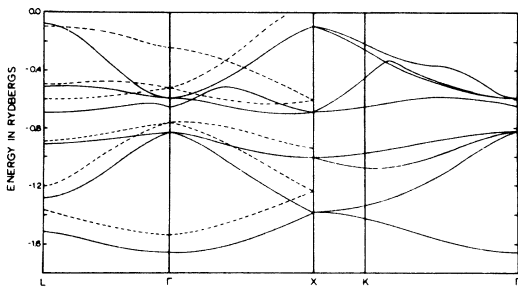


FIG. 6. Energy band structure of silicon with OAP. The solid curves were calculated by the tight-binding method with the  $1s$ -to- $3d$  basis set. The dashed curves are the OPW results of Ref. 15.

TABLE IV. Comparison between the modified scheme of OPW and tight-binding calculations of the  $\Gamma$ -point energies of Si (in a.u.).

	Tight binding		OPW (core states included)		
	$1s3d$	Extended basis	113	459	609
$\Gamma_1$	-0.829	-0.845	-0.837		-0.855
$\Gamma'_{25}$	-0.414	-0.431	-0.442	-0.455	-0.457
$\Gamma'_2$	-0.325	-0.334	-0.292	-0.327	-0.339
$\Gamma_{15}$	-0.294	-0.313	-0.319	-0.334	-0.335

crystal Hamiltonian. For our calculation the "approximate core functions" were taken as Bloch sums formed from the  $1s$ ,  $2s$ , and  $2p$  wave functions of the free atoms. These "approximate core functions" were not assumed to be the solution of the crystal Hamiltonian, consequently the matrix elements between two OPW's have to be computed by evaluating all integrals involving two plane waves, involving a plane wave and a localized atomic orbital, and involving two atomic orbitals on the same or different centers. With this procedure it is no longer necessary to use the "core shifts." The crystal wave function is expanded in terms of the basis set which consists of all the "approximate core functions" as well as the OPW's. The advantage of retaining all the "approximate core functions" in the basis set is that the roots of the secular equation now converge exactly to the true eigenvalues of the periodic-potential problem and, like the solutions of the tight-binding scheme, give upper limits to the energies of the one-electron Hamiltonian. Table IV gives the energies of the  $\Gamma$  point calculated using different numbers of OPW's. One may notice that with 113 OPW's, the  $\Gamma'_2$  state is above  $\Gamma_{15}$ , but the order is reversed when 609 OPW's are included. While the energy of  $\Gamma_{15}$  appears to have stabilized at 459 OPW's, the  $\Gamma'_2$  state still shows an appreciable change of energy from 459 to 609 OPW's. Although the  $\Gamma'_2$  energy may possibly decrease slightly beyond 609 OPW's, this point will not be pursued further as a detailed study of the convergence of this OPW calculation is beyond the scope of this paper. The tight-binding energies ( $1s$ -to- $3d$  basis) lie appreciably above the results of 609 OPW's. We have extended the tight-binding basis set by allowing the weightings of the individual STO in the  $1s$ ,  $2s$ ,  $2p$ ,  $3s$ ,  $3p$  Hartree-Fock functions to vary (similar to the calculations of diamond described in Sec. II B). The results of this extended basis set (Table IV) are slightly higher than the 609-OPW energies, and the differences give us some idea of the accuracy of tight-binding method as compared to a very elaborate OPW calculation.

In addition to Bassani and Yoshimine, several

other investigators have determined the band structure of silicon by the method of OPW. Two of these are self-consistent calculations of Stukel and Euwema<sup>6</sup> and the empirically adjusted SCF work of Herman *et al.*<sup>3-5</sup> A comparison with these results at high-symmetry points ( $\Gamma'_{25}$  set equal to zero) is given in Table V. Since the potentials used in these two calculations differ considerably from that of our OAP, only a qualitative comparison is meaningful. All three calculations are in good qualitative agreement and it is interesting that the LCAO, the modified OPW given in the preceding paragraph, and the SCF-OPW calculation of Stukel and Euwema predict  $\Gamma'_2$  to be below  $\Gamma_{15}$  - a result which disagrees with the previously published works.

#### IV. SODIUM

In view of the success of the application of the method of tight binding to lithium, it is interesting to investigate the case of sodium. Like the work of Schlosser and Marcus,<sup>31</sup> we adopt a muffin-tin crystal potential. The Wigner-Seitz cell is divided

into two regions by an inscribed sphere inside which the Prokofjew potential<sup>32</sup> was used. Between the inscribed sphere and the Wigner-Seitz cell, the potential is taken as a constant  $\bar{V}$  equal to the average of the Prokofjew potential in this region. Furthermore, in calculating  $\bar{V}$ , we have replaced the Wigner-Seitz cell by the equivalent volume sphere. This crystal potential is then expressed as a Fourier series over the crystal lattice with  $a_0 = 8.0426$  a.u. If the origin is chosen on an atomic site, this Fourier series contains only terms like  $\cos \vec{k} \cdot \vec{r}$ . The Fourier coefficients of this potential agree very well with those given by Schlosser and Marcus.<sup>31</sup>

The numerical Hartree-Fock SCF atomic wave functions of sodium for the 1s, 2s, 2p, 3s, and 3p states have been given by Fock and Petrashen,<sup>33</sup> and that for the 3d state has been calculated by the Hartree-Fock-Slater scheme.<sup>34</sup> For convenience of the numerical work, these wave functions are expressed as linear combinations of eight STO by means of curve fitting as follows:

$$\begin{aligned}
 \varphi_{1s} &= 7.1801 s_1 + 12.6244 s_2 + 0.038007 r s_3, \\
 \varphi_{2s} &= -1.115789 s_1 + 5.7947 s_2 - 6.4714 r s_3 - 1.47257 r s_4 - 0.011826 r^2 s_5 + 0.00158 r^2 s_6, \\
 \varphi_{3s} &= -0.2416 s_1 + 1.04212 s_2 - 1.19055 r s_3 - 0.285416 r s_4 + 0.0750607 r^2 s_5 + 0.034495 r^2 s_6, \\
 \varphi_{2px} &= x(7.1376 s_1 - 5.2863 s_2 + 0.14702 s_3 + 4.44533 s_4 + 14.0496 s_7), \\
 \varphi_{3px} &= x(-1.85643 s_1 + 2.0223 s_2 + 0.72637 s_3 - 0.56913 s_4 + 0.02624 r s_5 + 0.014757 r s_6 \\
 &\quad - 2.37233 s_7 + 0.019099 r s_8), \\
 \varphi_{3dxy} &= xy(0.071688 s_5 - 0.075850 s_6 + 0.091190 s_7 + 0.052076 s_8),
 \end{aligned} \tag{17}$$

where

$$s_i = e^{-\xi_i r}$$

and  $\xi_1$  to  $\xi_8$  are, respectively, 13.1474, 9.71542, 3.90983, 2.60387, 1.25944, 0.75485, 5.49636, 0.541733. Corresponding to each atomic orbital, a Bloch sum  $b_{nlm}(\vec{k}, \vec{r})$  can be formed. Since there is only one atom in a unit cell of the sodium crystal, the Bloch sums themselves, rather than their bonding and antibonding combinations as in the cases of diamond and silicon, are used as the basis functions. The energy band structure calculated by these fourteen basis functions is shown in Table VI. It is necessary to keep the 3d states in the basis set, because with only one atom per unit cell, the d orbitals are needed to form functions of  $H_{12}$  symmetry. In fact, if the 3d Bloch sums were deleted, the  $\Delta_1$  band curve would joint to the edge of the Brillouin zone at  $H_{15}$  (p-type symmetry) instead of  $H_{12}$ . As a test calculation, we have computed the tight-binding band structure by dropping the 3d state (see Table VI).

Except at the points near the zone edge H, the energy values along  $\Delta$ ,  $\Sigma$ , and  $\Lambda$  derived from the abridged basis set differ from those associated with the 1s-2s-2p-3s-3p-3d set by no more than 0.004 a.u.

Table VI also shows the comparison between the tight-binding results with the APW-type calculations of Schlosser and Marcus.<sup>31</sup> The agreement is seen to be quite good, i.e., within 0.01 a.u. except at the  $\Gamma$  point where the tight-binding value is 0.015 a.u. above that of Schlosser and Marcus. For  $\vec{k} = 0$ , our trial function is a linear combination of the 1s, 2s, and 3s Bloch sum. In other words, we have only two degrees of freedom in performing the linear variation calculation leading to the secular equation, whereas for a point on the  $\Delta_1$  line, say (0.2, 0, 0), there are four degrees of variational freedom. The lack of sufficient degree of flexibility of this trial function to reproduce the true crystal wave function at  $\Gamma$  point may be responsible for the discrepancy of 0.015 a.u. To pursue this point, we have generated a Bloch sum from an s-type atomic

TABLE V. Comparison of band structure of silicon calculated by different methods with different potentials (in a.u.).<sup>a</sup>

	TB OAP <sup>b</sup>	OPW <sup>c</sup>	OPW <sup>d</sup>	OPW <sup>e</sup>
	1s 3d	OAP	SCF-PERT	SCF
$\Gamma_1$	-0.414	-0.39	-0.430	-0.432
$\Gamma'_{25}$	0.0	0.0	0.0	0.0
$\Gamma'_{15}$	0.120	0.11	0.107	0.103
$\Gamma'_2$	0.090	0.25	0.153	0.101
$X_1$	-0.277	-0.25	-0.280	-0.285
$X_4$	-0.086	-0.09	-0.103	-0.100
$X_1$	0.073	0.07	0.046	0.047
$X_3$	0.367		0.395	0.360
$L'_2$	-0.342	-0.30	-0.346	-0.350
$L_1$	-0.229	-0.22	-0.248	-0.248
$L_4$	-0.038	-0.07	-0.043	-0.043
$L_3$	0.158	0.08	0.140	0.141
$L_1$	0.069	0.12	0.081	0.059
$L'_2$	0.375	0.32	0.317	

<sup>a</sup>In this table the energy of  $\Gamma'_{25}$  is set to zero.

<sup>b</sup>This work. TB refers to tight binding.

<sup>c</sup>Reference 15.

<sup>d</sup>Reference 4.

<sup>e</sup>Reference 6.

function composed of the same STO with the same weighting as in the Hartree-Fock-Slater 3d wave function, i.e.,

$$\phi_s = r^2(0.071688s_5 - 0.075850s_6 + 0.091190s_7 + 0.052076s_8), \quad (18)$$

and include this Bloch sum along with the 1s-2s-3s basis to recalculate the  $\Gamma$ -point energy. This gives -0.298 a.u. which is only 0.006 a.u. higher than the Schlosser-Marcus value. It is clear that this discrepancy can be further reduced by using a larger basis set for the tight-binding calculation.

A plot of the crystal wave function of the  $\Gamma$  point of the conduction band along the [100] line of the crystal lattice between two adjacent atoms is displayed in Fig. 7. The wave function is nearly constant over a large portion of the graph. It is interesting to note that by merely placing the atomic wave functions (in this case 1s, 2s, and 3s) at the proper sites, we automatically generate a crystal wave function which exhibits the constant electron-density property of a free particle. This occurs because of the strong overlap between the valence-electron wave functions of the neighbor atoms so that the valence electrons cannot be associated with a particular atom. When this overlap behavior is properly taken into account, the LCAO scheme of description gives energy band structures which agree quantitatively with those of the APW-type calculations. The same kind of results was also found for lithium.<sup>1,2</sup>

The steeply decreasing part of the wave function

TABLE VI. Energies (in a.u.) of the conduction band of sodium calculated by the tight-binding method with and without the 3d basis functions and their comparison with the results of the composite-wave method by Schlosser and Marcus ( $a_0 = 8.0426$  a.u.).

	Tight binding		Composite waves
$a_0 k_x / 2\pi$	1s 3d	1s 3p	(Ref. 31)
[000] $\Gamma$	-0.289	-0.289	-0.304
[100] $\Delta_1$			
0.2	-0.283	-0.280	-0.291
0.5	-0.213	-0.212	-0.224
0.8	-0.099	-0.095	-0.105
0.9	-0.053	-0.040	-0.056
1.0	-0.009( $H_{12}$ )	-0.003( $H_{15}$ )	-0.010
[110] $\Sigma_1$			
0.1	-0.289	-0.287	-0.297
0.3	-0.235	-0.234	-0.246
0.5	-0.147	-0.147	-0.147
[111] $\Lambda_1$			
0.1	-0.287	-0.283	-0.294
0.3	-0.207	-0.206	-0.218
0.5	-0.077	-0.075	-0.077

in Fig. 7 is due to the contribution of the 1s and 2s orbitals, whereas the 3s is mainly responsible for the flat portion. Also included in the same figure is the 3s Bloch sum which is essentially flat over the major part of the graph and decreases only mildly near the atomic sites. It is interesting to note from Fig. 7 that the Bloch sums of the 4s and 5s atomic states of sodium are practically identical to each other and are essentially constant over the entire region. These functions are not effective in providing variational freedom to the trial wave functions, and therefore their inclusion in the

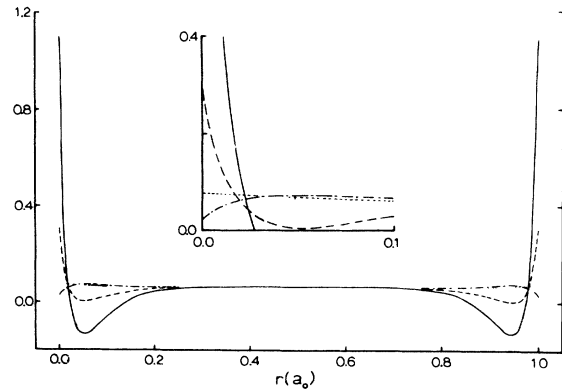


FIG. 7. Crystal wave function and Bloch sums at the  $\Gamma$  point of sodium along the [100] line of the crystal. The solid curve is the crystal wave function, and the 3s, 4s, 5s Bloch sums are presented by uniform dashes, long-short dashes, and dots, respectively.

basis set would not lower the energy substantially.

#### V. GENERALIZATION OF METHOD OF TIGHT BINDING

If we regard the method of tight binding as basically a linear variation method for calculating energies of a one-electron periodic-potential problem, an obvious way of improving the accuracy is to employ a trial function which resembles more closely the true wave function or to increase the number of basis functions used. In the calculation of diamond with the  $1s-2s-2p$  set ( $10 \times 10$ ), the wave function of  $\Gamma_1$  (and  $\Gamma'_2$ ) is written as a linear combination of bonding (and antibonding)  $1s$  and  $2s$  Bloch sums, or has only one degree of freedom, whereas the  $\Gamma_{15}$  and  $\Gamma'_{25}$  functions are of  $2p$  type having no variational freedom. It is interesting to note that even with such a limited degree of variational freedom, the tight-binding method is capable of giving quite accurate results. In Sec. IIE we have seen that augmentation of the basis set by means of the Bloch sums of the higher atomic orbitals is not fruitful. The Bloch sums formed by the successive higher orbitals tend to duplicate one another to a very large degree (Fig. 7), and do not provide the necessary variational freedom to improve the energy. Furthermore, the long range of the higher orbitals renders the crystal-lattice summation, e.g., Eq. (7) of Ref. 1, very difficult, and the labor of calculation increases immensely as the atomic orbitals become more diffuse.

A more practical and rewarding approach to acquire more flexibility of the trial function is to add to the basis-set Bloch sums generated by relatively localized atomiclike functions of ranges smaller than or comparable to the distance between two neighboring atoms in the crystal. By selecting a series of atomiclike functions which vary significantly over different portions of the region between a given atomic site and its nearest neighbors, it should be possible to reproduce quite accurately the true crystal wave functions in terms of the Bloch sums of such localized functions. For example, one can use the GTO of  $s$ -symmetry like  $e^{-\alpha_s r^2}$  and of  $p$ -symmetry like  $x e^{-\alpha_p r^2}$  to form the single-Gaussian Bloch sums as was done in Ref. 2. These single-Gaussian Bloch sums may be introduced to the basis set to supplement the regular Bloch sums of Hartree-Fock orbitals of the free atoms. Alternatively, we can adopt a basis set consisting entirely of single-Gaussian Bloch sums without ever using the conventional Bloch sums of the SCF atomic orbitals. In other words, in constructing the Bloch sums

$$B_n(\vec{k}, \vec{r}) = \sum_{\nu} e^{i\vec{k} \cdot \vec{R}_{\nu}} \chi_n(\vec{r} - \vec{R}_{\nu}),$$

the function  $\chi(\vec{r})$  is no longer restricted to the Hartree-Fock wave functions of the free atoms;

instead, any localized functions, in principle, may be used provided there are sufficient number of such basis functions to give the necessary variational freedom. The choice of the analytic form of  $\chi(\vec{r})$  is dictated by the ease of computation, and our previous work indicates that the Gaussian forms are suitable for this purpose. It is, of course, possible to take  $\chi(\vec{r})$  as the STO  $e^{-\zeta r}$  or as any arbitrary linear combinations of STO of different exponents, and indeed, we have essentially done the former in Sec. IIB in connection with augmenting the secular equation from  $10 \times 10$  to  $20 \times 20$ , and the latter in Sec. IV when we formed the Bloch sum corresponding to  $\varphi_s$  in Eq. (18). However, the multicenter integrals involving the Slater-type orbitals are more difficult to evaluate than their Gaussian counterparts. When dealing with a large number of Bloch-sum basis functions, the Gaussian form is more preferable.

As a preliminary calculation along this direction, we have added single-Gaussian Bloch sums of two  $s$ -type GTO ( $\alpha_s = 5.14773$  and  $0.49624$ ) and of three  $p$ -type GTO ( $\alpha_p = 1.14293$ ,  $0.35945$ , and  $0.1146$ ) to the usual  $1s$ ,  $2s$ , and  $2p$  Bloch sums of diamond. This makes a set of 32 basis functions which along with the muffin-tin potential of diamond gives the energies of the various points in the Brillouin zone as follows:  $\Gamma_1$ ,  $-1.148$ ;  $\Gamma'_{25}$ ,  $-0.433$ ;  $\Gamma_{15}$ ,  $-0.218$ ;  $\Gamma'_2$ ,  $-0.026$ ;  $X_1$ ,  $-0.856$ ;  $X_4$ ,  $-0.631$ ;  $X_1$ ,  $-0.201$ ;  $X_3$ ,  $0.086$ ;  $L'_2$ ,  $-0.958$ ;  $L_1$ ,  $-0.863$ ;  $L_4$ ,  $-0.523$ ;  $L_1$ ,  $-0.127$ ;  $L_3$ ,  $-0.112$ ;  $L'_2$ ,  $0.098$  a.u. Of special interest is the fact that the two largest discrepancies in energy (which occur at  $L'_2$  and  $X_1$ ) between the tight-binding and APW calculation, as shown in Fig. 1, are reduced to less than half of their values when we use the 32-basis set. The energies obtained from this basis set are on the average about 0.01 a.u. higher than the APW values. A detailed account of the methods of calculation using augmented basis sets of single-Gaussian Bloch sums will be reported in a later paper.

#### VI. CONCLUSION

The method of tight binding has been applied to calculate the band structures of diamond, sodium, and silicon. In the conventional sense of this method, we use the Hartree-Fock wave functions of the core states and of the occupied valence shells of the free atoms to form the Bloch sums, and expand the crystal wave function in terms of these Bloch sums. One obvious advantage of this scheme is that it entails a rather small number of basis functions (compared to some of the other first-principle methods such as OPW and APW) and at the same time achieves reasonably good accuracy. Furthermore, since the crystal wave functions are expressed in terms of the wave functions of the

constituent atoms, it is possible to make more direct correlation between the properties of the crystals and those of the free atoms on both quantitative and qualitative level. If the atomic Hartree-Fock functions are expressed in terms of a small number of Slater-type orbitals, one can improve the calculation somewhat by varying their relative weightings to minimize the energy. For sodium, this tight-binding procedure leads to band energies accurate to typically 0.02 Ry. In the case of diamond and silicon, the average error is estimated to be 0.04 Ry.

To obtain band structure of higher accuracy, modifications and generalization of the method of tight binding can be readily made. In generating the Bloch sums, one may replace the atomic Hartree-Fock functions by a series of GTO of various ranges. These single-Gaussian Bloch sums are then included in the basis set for the secular equation. Even with a modest increase of the number of basis functions, we have improved the accuracy of the tight-binding calculations for diamond to generally 0.02 Ry. The matrix elements of the Hamiltonian

between two single-Gaussian Bloch sums can be expressed in analytic form and no numerical integration is needed. Our results demonstrate that the method of tight binding is capable of giving very accurate results. The success of this method in both alkali metals and group-IV crystals points toward the possibility of application to a wide variety of materials.

#### ACKNOWLEDGMENTS

The authors wish to express their appreciation to Preston E. Chaney and Mrs. Barbara Lafon for their invaluable assistance and continual interest in this research. We also gratefully acknowledge the support of the University of Wisconsin Research Committee and of the Oklahoma State University Research Foundation for computer usage, and the assistance rendered by the University of Wisconsin Computer Center and the Oklahoma State University Computer Center. One of us (R.C.C.) is especially grateful to the Sun Oil Company for making their computer facilities available to him.

\*Work supported in part by the U.S. Office of Naval Research.

†Present address: University of Texas at Dallas, Dallas, Tex. 75230.

<sup>1</sup>E. E. Lafon and C. C. Lin, *Phys. Rev.* **152**, 579 (1966).

<sup>2</sup>R. C. Chaney, T. K. Tung, C. C. Lin, and E. E. Lafon, *J. Chem. Phys.* **52**, 361 (1970).

<sup>3</sup>F. Herman, R. L. Kortum, C. D. Kuglin, and R. A. Short, *J. Phys. Soc. Japan Suppl.* **21**, 7 (1966).

<sup>4</sup>F. Herman, R. L. Kortum, and C. D. Kuglin, *Int. J. Quantum Chem.* **15**, 533 (1967).

<sup>5</sup>F. Herman, R. L. Kortum, C. D. Kuglin, and R. A. Short, in *Quantum Theory of Atoms, Molecules, and Solid State*, edited by P.-O. Löwdin (Academic, New York, 1966), p. 381.

<sup>6</sup>D. J. Stukel and R. N. Euwema, *Phys. Rev. B* **1**, 1635 (1970).

<sup>7</sup>R. Keown, *Phys. Rev.* **150**, 568 (1966).

<sup>8</sup>L. F. Mattheiss, *Phys. Rev.* **133**, A1399 (1964); **134**, A970 (1964); **139**, A1893 (1965).

<sup>9</sup>J. C. Slater, *Phys. Rev.* **81**, 385 (1951).

<sup>10</sup>P. M. Scop, *Phys. Rev.* **139**, A934 (1965).

<sup>11</sup>F. Herman and S. Skillman, in *Proceedings of the International Conference on Semiconductor Physics, Prague, 1960* (Publishing House of Czechoslovak Academy of Sciences, Prague, 1961), p. 20; D. J. Stukel, R. N. Euwema, T. C. Collins, F. Herman, and R. L. Kortum, *Phys. Rev.* **179**, 740 (1969).

<sup>12</sup>T. O. Woodruff, *Solid State Phys.* **4**, 367 (1957).

<sup>13</sup>A. Jucys, *Proc. Roy. Soc. (London)* **A175**, 59 (1939).

<sup>14</sup>Instead, one may consider the individual atoms to be in their "valence state"  $(1s)^2(2s)(2p)^3$  and calculate the potential accordingly. We chose  $(1s)^2(2s)^2(2p)^2$  here in order that we can compare our results with those of the OPW calculations by Bassani and Yoshimine (Ref. 15).

<sup>15</sup>F. Bassani and M. Yoshimine, *Phys. Rev.* **130**, 20

(1963).

<sup>16</sup>E. R. Keown and J. H. Wood, MIT Solid State and Molecular Theory Group Quarterly Progress Report No. 53, 1964 (unpublished).

<sup>17</sup>A. Jucys, *J. Phys. (USSR)* **11**, 49 (1947).

<sup>18</sup>C. D. Clark, P. J. Dean, and P. V. Harris, *Proc. Roy. Soc. (London)* **A277**, 312 (1964).

<sup>19</sup>P. J. Dean and E. C. Lightowers, *Phys. Rev.* **140**, A352 (1965).

<sup>20</sup>See footnote 3 of Ref. 7 for a list of the earlier works on the band structure of diamond.

<sup>21</sup>E. Lafon, MIT Solid State and Molecular Theory Group Quarterly Progress Report No. 69, p. 66, 1968 (unpublished).

<sup>22</sup>I. Goroff and L. Kleinman, *Phys. Rev.* **164**, 1100 (1967).

<sup>23</sup>R. M. Raccach, R. N. Euwema, D. J. Stukel, and T. C. Collins, *Phys. Rev. B* **1**, 756 (1970).

<sup>24</sup>S. Göttlicher and E. Wölfel, *Z. Elektrochem.* **63**, 891 (1959).

<sup>25</sup>R. H. Parmenter, *Phys. Rev.* **86**, 552 (1952).

<sup>26</sup>F. Herman and S. Skillman, *Atomic Structure Calculations* (Prentice-Hall, Englewood Cliffs, N. J., 1963).

<sup>27</sup>S. Huzinaga, *J. Chem. Phys.* **42**, 1243 (1965).

<sup>28</sup>E. Clementi, *IBM J. Res. Develop.* **9**, 2 (1965), and the supplement to this paper.

<sup>29</sup>A. Frova and P. Handler, *Phys. Rev. Letters* **14**, 178 (1965).

<sup>30</sup>G. Feher, *Phys. Rev.* **14**, 1219 (1959).

<sup>31</sup>H. Schlosser and P. M. Marcus, *Phys. Rev.* **131**, 2529 (1963); H. Schlosser, Ph.D. thesis, Carnegie Institute of Technology, 1960 (unpublished).

<sup>32</sup>W. Prokofjew, *Z. Physik* **58**, 255 (1929). Discontinuities were found at the boundaries between some of the regions of the potential as expressed in polynomial form in Table I of this reference. These discontinuities can be removed by changing the coefficient  $-0.0264$  in

the second region to  $-0.00264$  and the coefficient  $-1.508$  in the fourth region to  $1.508$ . These changes were adopted in our calculations.

<sup>33</sup>V. Fock and M. Petrashen, *Physik Z. Sowjetunion* 6, 368 (1934).

<sup>34</sup>D. F. Korff (private communication).